



Published in final edited form as:

Nature. 2019 March ; 567(7746): 127–131. doi:10.1038/s41586-019-0990-0.

Structural basis for KCTD-mediated rapid desensitization of GABA_B signaling

Sanduo Zheng¹, Nohely Abreu², Joshua Levitz², and Andrew C. Kruse¹

¹Department of Biological Chemistry and Molecular Pharmacology, Harvard Medical School, Boston, MA, USA.

²Department of Biochemistry, Weill Cornell Medicine, New York, NY, USA.

Abstract

The GABA_B receptor is one of the principal inhibitory neurotransmitter receptors in the brain, and it signals through heterotrimeric G proteins to activate a variety of effectors including G protein-coupled inwardly-rectifying potassium channels (GIRKs)^{1,2}. GABA_B receptor signaling is tightly regulated by auxiliary subunits called KCTDs, which control the kinetics of GIRK activation and desensitization^{3–5}. However, the mechanistic basis for KCTD modulation of GABA_B signaling remains incompletely understood. Here, using a combination of X-ray crystallography, electron microscopy, functional and biochemical experiments we reveal the molecular details of KCTD binding to both GABA_B receptors and Gβγ subunits. KCTDs associate with the receptor by forming an asymmetric pentameric ring around a region of the receptor C-terminal tail, while a second KCTD domain, H1, engages in a symmetric interaction with five copies of Gβγ in which the G protein subunits also directly interact with one another. We further show that KCTD binding to Gβγ is highly cooperative, defining a model in which KCTDs cooperatively strip G proteins from GIRK channels to induce rapid desensitization following receptor activation. These results provide a framework for understanding the molecular basis for the precise temporal control of GABA_B signaling by KCTD proteins.

The GABA_B receptor (GABA_BR) is expressed in excitatory and inhibitory synapses throughout the brain, and it is an important target for anxiolytic and antispastic drugs^{1,2}. The receptor is a heterodimer composed of GABA_{B1} and GABA_{B2} subunits, both of which are essential for the formation and trafficking of a functional receptor⁶. Upon activation, the receptor catalyzes dissociation of heterotrimeric G proteins into Gα_{i/o} and Gβγ subunits to initiate downstream signaling^{7,8}. Following activation of presynaptic GABA_BRs, the Gβγ heterodimer typically inhibits voltage-gated calcium channels (VGCCs) to suppress

Reprints and permissions information is available at <http://www.nature.com/reprints>. Users may view, print, copy, and download text and data-mine the content in such documents, for the purposes of academic research, subject always to the full Conditions of use: http://www.nature.com/authors/editorial_policies/license.html#terms

Correspondence and requests for materials should be addressed to A.C.K. (andrew.kruse@hms.harvard.edu).

Author Contributions S.Z. performed protein purification, biochemical assays, and structural studies by crystallography and negative stain electron microscopy, with supervision from A.C.K. Electrophysiology and microscopy experiments were performed by N.A. with supervision from J.L. The manuscript was written by S.Z. and A.C.K. with input from N.A. and J.L.

Supplementary Information is available in the online version of the paper

The authors declare no competing interests.

neurotransmitter release, while activation of postsynaptic GABA_BRs usually activates outward potassium conductance via G protein-coupled inwardly rectifying potassium channels (GIRKs)^{9–11} to generate slow inhibitory postsynaptic currents (sIPSCs)^{11,12}.

GABA_B signaling is controlled by the proteins KCTD8, KCTD12, and KCTD16, which serve as auxiliary receptor subunits that regulate the rise time and duration of GIRK currents and enhance receptor expression levels^{3–5}. These effects are mediated by KCTD interaction with the GABA_{B2} receptor C-terminus and with Gβγ proteins^{4,13}. KCTDs are genetically associated with mood disorders including bipolar disorder¹⁴, and their heterogeneous subtype expression patterns serve to create pharmacologically distinct populations of GABA_B receptors in different brain regions¹⁵. Despite their importance, the mechanisms of KCTD receptor binding and G protein sequestration are ill-defined. Here, we sought to tackle these problems to define the structural and mechanistic basis for KCTD function.

KCTDs 8, 12, and 16 consist of an N-terminal BTB domain followed by a region of unknown structure termed the “H1” domain. The BTB domain mediates binding to GABA_B receptors at the distal receptor tail centered around GABA_{B2} Tyr903 (we use human sequence numbering throughout; this residue is equivalent to Tyr902 in mouse)^{13,16}. We sought to identify a GABA_{B2} peptide fragment capable of binding to a KCTD protein. We found that a peptide consisting of GABA_{B2} residues 876 – 913 was capable of binding to KCTD16_{BTB} (Fig. 1a and Extended Data Fig. 1a and 1b), and we determined the crystal structure of this peptide in complex with KCTD16_{BTB} to 3.2 Å resolution (Fig. 1b and Extended Data Table 1 and Extended Data Fig. 2).

The structure shows an unusual overall architecture, with KCTD16_{BTB} adopting an asymmetric pentameric arrangement and wrapping around the GABA_{B2} C-terminus (Fig. 1b). While previous reports suggested that KCTD16 functions as a tetramer, both our structure and a recently reported peptide-free KCTD16_{BTB} structure showed a pentameric arrangement¹⁷ (Extended Data Fig. 1c). Over a stretch of roughly 25 amino acids, nearly every side chain in the GABA_{B2} tail interacts with KCTD16_{BTB} (Fig. 1b). Within the interface, KCTD16_{BTB} residue Phe80 makes particularly extensive contacts with the peptide in each of the five subunits (Fig. 1c). Confirming the importance of these interactions, we found that an F80A mutation caused a complete loss of GABA_{B2} peptide binding activity *in vitro* (Extended Data Fig. 1d), and an equivalent substitution in KCTD12 resulted in loss of GABA_B-mediated KCTD12 membrane localization in cells (Fig. 1d). Almost all residues in the interaction interface are conserved in all GABA_B-regulating KCTD subtypes (KCTD8, KCTD12 and KCTD16), accounting for the specific binding of these KCTDs for GABA_B receptor (Extended Data Fig. 1e).

In addition to binding the GABA_{B2} receptor tail, KCTDs also interact with Gβγ subunits⁴. In an *in vitro* pull-down assay with GST-tagged KCTD12 we found that a sub-stoichiometric amount of GABA_{B2} receptor tail but near stoichiometric amounts of Gβ₁γ₂ heterodimer could be pulled down by KCTD12. In contrast, KCTD12 failed to co-purify Gαβγ heterotrimer irrespective of Gα subtype (Fig. 2a and Extended Data Fig. 3a and 3b). While the KCTD12 BTB domain mediates interaction with the receptor, its C-terminal H1 domain is responsible for desensitization¹⁸. Consistent with this, we observed that the KCTD12 H1

domain alone was sufficient to bind $G\beta\gamma$ with an affinity of 185 nM (Fig. 2b; Extended Data Figure 3c). Negative stain electron microscopy (EM) 2D class averages of KCTD12_{H1} in complex with $G\beta\gamma$ revealed a symmetric pentameric assembly with the H1 domain pentamer engaging in interaction with five copies of $G\beta\gamma$ heterodimer (Fig. 2b and Extended Data Fig. 3d–f).

To investigate the details of H1 domain interaction with $G\beta\gamma$ in more detail, we determined the crystal structure of the KCTD12_{H1}/ $G\beta\gamma$ complex to 3.7 Å resolution (Extended Data Table 1 and Extended Data Fig. 2b). In parallel, we also determined a negative-stain EM envelope for full-length KCTD12 in complex with $G\beta\gamma$ (**Extended Data 4**). These data showed that the KCTD12_{H1}/ $G\beta\gamma$ complex is pentameric and shows near-perfect C5 symmetry. KCTD12_{H1} possesses a β -propeller-like fold, with each H1 domain comprising a separate blade of the propeller. The propeller is surrounded by a tightly packed ring of $G\beta\gamma$ heterodimers in direct contact with one another. Interactions between KCTD12 and the G protein are confined to the $G\beta$ subunit, with $G\gamma$ subunits peripherally arrayed around the edge of the pentameric ring (Fig. 2c). Previous reports had suggested that the motif NFLEQ in KCTD12 is important for receptor desensitization¹⁸. However, in the crystal structure this region does not interact with $G\beta\gamma$ subunits, but instead is involved in oligomeric contacts between adjacent KCTD12 subunits (Extended Data Fig. 5a).

The KCTD12 H1 domain itself consists of a five-stranded antiparallel β -sheet interrupted by two α helices (Extended Data Fig. 5b). The five $G\beta\gamma$ subunits each interact with two KCTD12_{H1} subunits, which together occlude a large surface on $G\beta$ (Fig. 3a and Extended Data Fig. 5c). The loop between the first and second β strands of KCTD12_{H1} includes basic residues which interact with an acidic patch on the $G\beta$ propeller (Fig. 3b), and a longer loop in KCTD12_{H1} after the first α helix sits in the groove between the N-terminal helix of $G\beta\gamma$ and the β propeller domain (Fig. 3c). Mutating residues in the KCTD12 H1 domain in either of these interfaces (R232D or R257D) entirely abolished G protein binding (Fig. 3d). Although both KCTD mutants can localize to the cell membrane in the presence of GABA_B receptors (Extended Data Fig. 5d), they fail to desensitize GABA_B-mediated GIRK channel currents (Fig. 3e and 3f). Interestingly, the KCTD binding site on the surface of $G\beta\gamma$ would partially occlude $G\alpha$ binding (Fig. 3g), but is entirely non-overlapping with the GIRK channel binding site (Fig. 3g and 3h)¹⁹. Hence, binding of a KCTD12 pentamer to a single $G\beta\gamma$ subunit in complex with GIRK2 could be accommodated with minimal structural rearrangement, although the full 5:5 complex is incompatible due to extensive clashes between the GIRK2 intracellular domain and other KCTD12-bound $G\beta\gamma$ dimers (Fig. 3h and Extended Data Fig. 6a and 6b).

One of the more remarkable features of the complex is the fact that $G\beta\gamma$ subunits pack so closely to one another that they interact directly, burying a 351 Å² surface. In contrast, the GIRK channel is bound by four spatially isolated $G\beta\gamma$ subunits (Extended Data Fig. 6a–c). Residues in the $G\beta$ - $G\beta$ interface observed in our structure are highly conserved across species, raising the possibility that this interaction is functionally important. To test this, we incubated KCTD12_{H1} with a substoichiometric amount of $G\beta\gamma$. Under these conditions, only full 5:5 complexes and free KCTD12 were seen in size exclusion chromatography, with no evidence of partial oligomers, suggesting that KCTD12 binding to $G\beta\gamma$ is highly

cooperative (Extended Data Fig. 6d). When a single G β residue involved in oligomeric G β -G β contacts was mutated (R42D), we observed a broad 5:5 complex peak and free G $\beta\gamma$ in size exclusion. Introduction of a second mutation (R46D) resulted in only partial complex formation (Extended Data Fig. 6e), further supporting a role of cooperative G β -G β contacts in KCTD binding.

G $\beta\gamma$ is the key signaling intermediate in GABA_B activation of GIRK currents, and in the course of a signaling event a G $\beta\gamma$ subunit sequentially interacts with a series of progressively higher affinity binding partners. The K_D 's for G $\beta\gamma$ binding to GTP-bound G α_i , GIRK channels, KCTD12, and GDP-bound G α_i are (in order): undetectable, ~250 μ M^{20,21}, 185 nM (**Extended Data 3c**), and 3 nM²². If G $\beta\gamma$ affinity for KCTDs is so much higher than for GIRK channels, how can KCTDs desensitize the channels without preventing their activation in the first place? Clearly the on rate for G $\beta\gamma$ association with KCTDs must be lower than that for association with GIRK channels, otherwise G $\beta\gamma$ subunits would be sequestered prematurely. We propose one possible explanation for how this might be achieved.

KCTDs bind at the distal C-terminus of the GABA receptor B2 subunit, roughly 350 Å from the last transmembrane domain with an intervening structurally rigid coiled-coil domain. This means that KCTDs can diffuse far from the membrane plane (Fig. 4). When the GABA_B receptor is activated, G $\beta\gamma$ subunits are liberated from G α but remain tethered to the membrane due to their lipid anchor, resulting in GIRK channel activation while KCTDs are at a relatively low local concentration. When a KCTD molecule happens to encounter a GIRK-bound G $\beta\gamma$ subunit it can bind simultaneously, but formation of the oligomeric complex is sterically incompatible with G $\beta\gamma$ binding to GIRK channels. The higher affinity and cooperativity of binding to KCTD may then drive stripping of subsequent G $\beta\gamma$ subunits from GIRKs following an initial encounter, resulting in rapid channel closure. Finally, reassociation of G $\beta\gamma$ with GDP-bound G α subunits could restore equilibrium and reset the cycle (**Extended Data 7**).

The regulation of GABA_B signaling by KCTD proteins is a unique and important means of achieving functional diversity in these critical receptors. Here we have shown how the KCTD BTB domain recognizes the GABA_{B2} C-terminus to tether a G $\beta\gamma$ -sequestering H1 domain on the receptor's distal tail, providing a means of efficiently deactivating GIRK channels. In this way KCTDs afford GABA_B receptors with tight temporal control of signaling not achievable with the slower β -arrestin pathway used to desensitize most GPCRs.

METHODS

Protein Expression and Purification

Human KCTD12 and KCTD16 genes were synthesized (Integrated DNA Technologies). KCTD12 (residues 32–131) and KCTD16 (residues 23–124) BTB domains were cloned into a pET28a expression vector (EMD Millipore) for the expression of an N-terminal His₆-SUMO fusion protein or an untagged version in *Escherichia coli* strain BL21(DE3). KCTD12 (residues 200–325) and KCTD16 (residues 158–279) H1 domain were cloned into

the multiple cloning site 1 of pETduet-1 vector (EMD Millipore) and expressed with an N-terminal His₆-SUMO tag followed by 3C protease site. All human GABA_{B2} C-terminal truncations were cloned into the same vector with an N-terminal His₆-GST or His₆-SUMO fusion protein followed by 3C protease site and were expressed in BL21(DE3) *E. coli*. KCTD12 (residues 32–325) and KCTD16 (residues 21–279) constructs containing both BTB and H1 domains were cloned into the vector pVL1393 vector (Expression Systems) and protein was expressed using baculovirus infection of Sf9 insect cells (Expression Systems) according the manufacturer's protocols. These constructs were expressed with an N-terminal His₆-GST fusion protein followed by a 3C protease site. Human Gα_q was cloned into pVL1393 without tags. Human Gβ₁γ₂ heterodimer was modified to include an N-terminal His₆ tag on the Gβ subunit and a C68S point mutation in Gγ, which eliminates the lipid modification site. A bicistronic vector based on pVL1392 was used to prepare baculovirus encoding both subunits. All point mutations and deletions were introduced by the QuikChange method.

Plasmids encoding untagged KCTD16 BTB and His₆-GST-tagged GABA_{B2} fragment were co-transformed into *E. coli* BL21(DE3) strain. Bacteria were cultured in LB medium supplemented with 50 μg ml⁻¹ ampicillin and 50 μg ml⁻¹ kanamycin at 37 °C to an OD₆₀₀ value of 0.8, and protein expression was induced by the addition of 0.5 mM isopropyl 1-thio-β-D-glucopyranoside followed by shaking overnight at 18 °C. Cells were harvested by centrifugation, resuspended in buffer A (50 mM Tris-HCl, pH 8.0, 250 mM NaCl and 25 mM Imidazole) and lysed by sonication. His-GST-GABA_{B2} fragment in complex with KCTD16_{BTB} was purified from clarified lysate by Ni-NTA affinity chromatography. Resin was washed with buffer A and protein then eluted with buffer B (50 mM Tris-HCl, pH 8.0, 250 mM NaCl and 250 mM Imidazole). The eluted fraction was incubated with 3C protease overnight to cleave His₆-GST tag. Protein solution was diluted three-fold by 20 mM HEPES-NaOH, pH 7.6 and loaded onto a Q sepharose column (GE Healthcare). The flow-through was collected, concentrated and further purified by size exclusion chromatography (SEC) Superdex S200 10/300 equilibrated in storage buffer (10 mM HEPES-NaOH pH 7.6, and 150 mM NaCl). Protein expression and nickel affinity purification for His₆-SUMO-tagged KCTD12 H1 was performed as described above. After tag cleavage by 3C protease, the protein sample was concentrated and purified on a Superdex S200 10/300 size exclusion column equilibrated in storage buffer.

His₆-GST-tagged KCTD12 32–325 or KCTD16 21–279 was expressed in Sf9 insect cell cultures using the BestBac baculovirus system (Expression Systems). Infection was performed when cells reached a density of 3 × 10⁶ cell per mL and flasks were shaken at 27 °C for 36 hours before harvest. Cells were harvested by centrifugation and lysed in buffer A using a glass dounce tissue grinder. Protein was purified by Ni-NTA gravity flow chromatography followed by glutathione agarose bead affinity purification (GE Healthcare). The protein was further purified by Superdex S200 10/300 equilibrated in storage buffer. His₆-tagged Gβ₁ and Gγ₂ (C68S mutant) were expressed in Sf9 insect cells using the BestBac system (Expression Systems) as described above. Purification was performed as previously reported²³.

For KCTD12_{H1}/Gβ₁γ₂ complex assembly and purification, individually purified KCTD12 H1 and Gβ₁γ₂ proteins were mixed in a 1:1.2 molar ratio and then incubated at room temperature for 30 min. Excess Gβ₁γ₂ was separated from KCTD12 H1/Gβ₁γ₂ complex on a Superdex S200 10/300 column in binding buffer (20 mM HEPES-NaCl pH 7.6 and 50 mM NaCl). For KCTD16 21–279/GABA_{B2} 876–913 complex, purified His6-SUMO-tagged GABA_{B2} 876–913 and His6-GST-tagged KCTD16 21–279 were mixed in a 2:1 molar ratio. The His6-SUMO tag of GABA_{B2} and His6-GST tag of KCTD16 21–279 were cleaved by 3C protease at 4°C overnight. The protein complex was further purified by SEC S200 10/300 with storage buffer. For KCTD12 32–325/GABA_{B2} 876–913/ Gβ₁γ₂ complex, individually purified His₆-GST-tagged KCTD12 32–325, His₆-SUMO-tagged GABA_{B2} 876–913, and Gβ₁γ₂ were mixed in a 1:2:1.2 ratio. After tag cleavage by 3C protease the protein sample was loaded onto Superdex S200 10/300 equilibrated in binding buffer.

GST pull-down assay

To identify a minimal portion of GABA_{B2} suitable for binding KCTDs, a series of GABA_{B2} C-terminal truncations were cloned. His6-SMT3 tagged KCTD12 or KCTD16 and His6-GST tagged GABA_{B2} truncation were co-transformed and co-expressed in *E. coli* BL21(DE3) strain. GST pull-down experiment was performed as previously described²⁴. For interaction analysis, individually purified His6-SUMO-tagged GABA_{B2} 876–913 or Gβ₁γ₂ complex or Gα_qβ₁γ₂ complex was added to His6-GST-tagged KCTD12 32–325 in an excessive amount in 200 μl of binding buffer. The mixtures were incubated with 20 μL of glutathione-Sepharose beads and gently rotated at 4 °C for 1 hour. After the beads were washed three times with binding buffer, the bound protein was eluted with 20 μL of binding buffer supplemented with 20 mM glutathione. Input and eluate samples were resolved using SDS-PAGE and stained with Coomassie Blue.

Crystallization and structure determination

The KCTD16 BTB domain (23–124) and GABA_{B2} fragment (876–913) were crystallized at 20 °C using the hanging-drop vapor diffusion method by mixing 0.5 μL of protein (19 mg mL⁻¹) and 0.5 μL of reservoir solution containing 100 mM MgCl₂, 100 mM Tris-HCl pH 7.5 and 12% (w/v) PEG8000. Initial efforts to crystallize the KCTD12 H1 domain in complex with Gβ₁γ₂ were only successful in wells with fungal contamination. Although these crystals did not diffract, we reasoned that trimming by fungal proteases might be facilitating crystallogenesis. Indeed, strongly diffracting crystals were obtained when purified KCTD12 H1 (200–325) and Gβ₁γ₂ were mixed in a 1:1.2 molar ratio with a small amount of trypsin (1:1000 by mass) for 30 min at room temperature prior to setting trays. Crystals were obtained by the sitting drop vapor diffusion method in drops mixed with 100 nL of protein (9 mg/ml⁻¹) and 100 nL of reservoir solution containing 0.2 M NaCl, 0.1 M sodium cacodylate and 8% (w/v) PEG8000 after overnight growth at 20 °C. The crystals were flash-frozen in liquid nitrogen without additional cryoprotection.

Diffraction data were collected at Advanced Photon Source GM/CA beamlines 23ID-B and 23ID-D with a 20 μm collimated beam dimension. Data were processed in HKL2000²⁵. Crystals for KCTD16_{BTB} in complex with the GABA_{B2} fragment complex belonged to the *P*₂₁ space group, and contained two copies of KCTD16 BTB-GABA_{B2} fragment complex

per asymmetric unit. Phase was determined with molecular replacement using *Phaser* in *Phenix*²⁶ with the KCTD16_{B₂TB} structure (PDB ID: 5A15)¹⁷ as a search model. The final refined structure includes two copies of KCTD16_{B₂TB} pentamer with residues 23–124 resolved, and two GABA_{B2} C-terminal peptides with residues 884–913 resolved. Ramachandran analysis showed that 95.7% of residues are in the favored regions, and 4.3% in the allowed regions. Crystals for KCTD12_{H1}/Gβ₁γ₂ complex belonged to space group *P*2₁2₁2₁. The structure was solved by molecular replacement using *Phaser* in *Phenix* with the structure of bovine Gβ₁γ₂ heterodimer (PDB ID: 1OMW)²⁷ as a search model. The final model includes one copy of KCTD12 H1 pentamer (residues, 206–324) and five copies of Gβ₁γ₂ complex. The model was refined through iterative model building in Coot²⁸ and reciprocal space refinement in *phenix.refine*²⁹. The final structure has 97.36% and 2.64% of residues in the favored and allowed regions of Ramachandran plot respectively.

Isothermal titration calorimetry

ITC experiments were performed with an ITC200 microcalorimeter (Microcal Inc.) at 30 °C. Purified KCTD12_{H1} and Gβ₁γ₂ were exchanged to the same buffer (20 mM HEPES-NaCl, pH 7.6 and 100 mM NaCl) with a HiTrap Desalting column (GE healthcare) before titration. 160 μM of Gβ₁γ₂ was injected via syringe into sample cell containing 16 μM of KCTD12_{H1}. The integrated heat data were analyzed using one-set-of-sites model in Origin according to the manufacturer's instructions. The dissociation constant K_D was calculated as $1/K_A$.

Electron microscopy and 3D reconstruction

For negative staining, 2.5 μL of protein solution consisting of a complex of GABA_{B2} C-terminal peptide, full-length KCTD12, and Gβ₁γ₂ at a concentration of ~0.01 mg/mL was added to a glow-discharged carbon-coated copper grid (Electron Microscopy Science) and allowed to adsorb for 20 seconds. Grids were then washed twice with deionized water and then stained twice with freshly prepared 0.75% (w/v) uranyl formate. Filter paper was applied to absorb residual liquid between each step.

Images were collected at room temperature using a Philips Tecnai T12 electron microscope equipped with an LaB6 filament and operated at 120 kV. Images were collected at a magnification of 52,000-fold and a defocus value of 1.5 μm on a Gatan 4K CCD using low-dose collection procedure. Particles were manually picked in Eman2³⁰ and 2D class averages were calculated with Relion³¹. 3D initial model building, 3D classification, and refinement were carried out in CisTEM³².

HEK 293T cell imaging

KCTD12 or mutants were cloned into pCDNA3.1 vector for the expression of an N-terminal protein C (PC-KCTD12) or eGFP fusion protein (eGFP-KCTD12). HEK 293T cells were cultured in Dulbecco's modified Eagle's medium (DMEM) supplemented with 5% Fetal Bovine Serum (FBS) and maintained at 37°C in a 5% CO₂ humidified incubator. Cells were seeded on poly-L-lysine coated 18 mm coverslips 18 hr before transfection. Transfections were done using Lipofectamine 3000 (Invitrogen) with 0.7 μg per well of eGFP-KCTD12,

eGFP-KCTD12-F87A, eGFP-KCTD12-R232D or eGFP-KCTD12-R257D with and without 0.5 μg each of GABA_{B1A} and GABA_{B2}.

Living cells were imaged at room temperature ($\sim 25^{\circ}\text{C}$) 42 hr after transfection in extracellular solution composed of 135 mM NaCl, 5.4 mM KCl, 10 mM HEPES, 2 mM CaCl₂, and 1 mM MgCl₂, pH 7.4. Imaging was performed on an Olympus IX-73 microscope using a 60 \times 1.49 NA APO N TIRFM objective (Olympus) and snapshots were taken with a sCMOS ORCA-Flash4 v3.0 camera (Hamamatsu). GFP was excited with a 488 nm laser diode. Images were saved as 16-bit TIFF files. An ROI was drawn around a blank area lacking cells to perform background-subtraction using a macro on Fiji (ImageJ) that subtracts the mean intensity value of the ROI from the image. Line-scan analysis was performed on background-subtracted images.

Whole-cell patch clamp electrophysiology

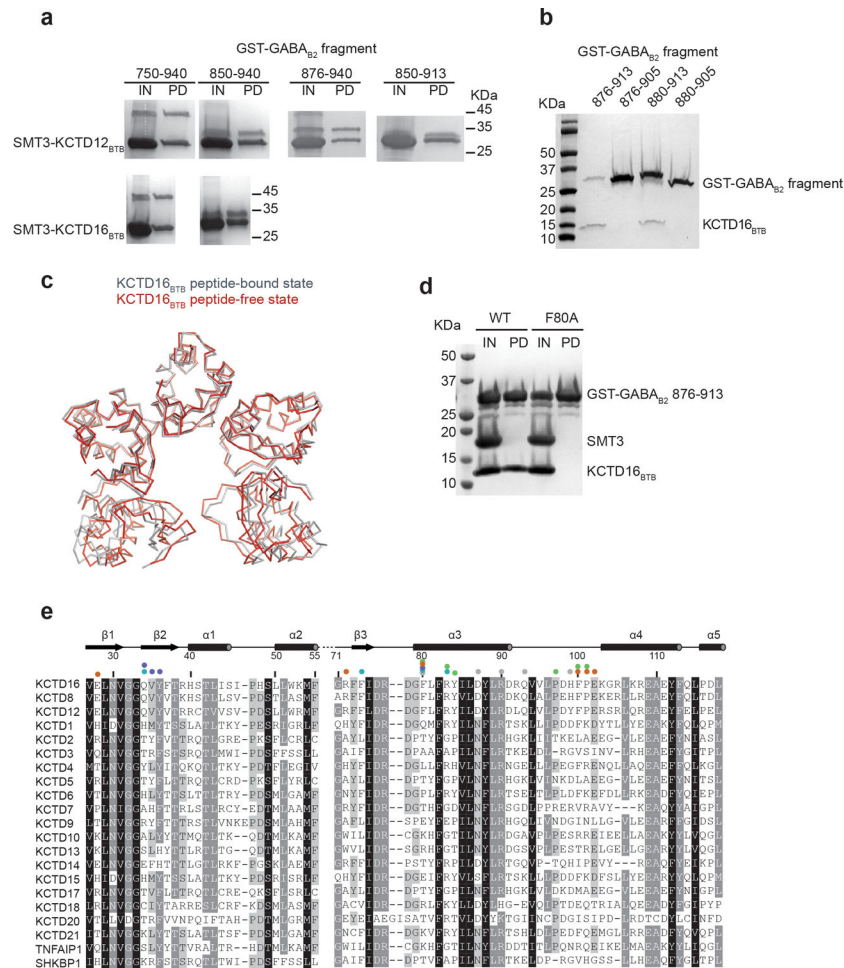
Chinese Hamster Ovary (CHO) cells were cultured in Nutrient Mixture F-12 Ham (Sigma-Aldrich) supplemented with 10% FBS, 14 mM Sodium Bicarbonate, and 11 mM D-Glucose (pH 7.2) and maintained at 37 $^{\circ}\text{C}$ in a 5% CO₂ humidified incubator. Cells were seeded on poly-L-ornithine coated 18 mm coverslips and transfected ~ 24 hr later. Transfections were done using Lipofectamine 2000 (Invitrogen) with 0.7 μg of either KCTD12, EGFP-KCTD12, EGFP-KCTD12-F80A, EGFP-KCTD12-R232D or EGFP-KCTD12-R257D, 0.7 μg GIRK1-F137S (homotetramerization mutant), 0.3 μg tdTomato, and 0.35 μg each of rat GABA_{B1A} and GABA_{B2}. Cells were maintained in 2 μM CGP 54626 post-transfection to reduce basal activity of GABA_B and maintain cell health.

Whole-cell patch clamp experiments were performed 42–72 hr after transfection in an extracellular solution containing 120 mM KCl, 25 mM NaCl, 10 mM HEPES, 2 mM CaCl₂, and 1 mM MgCl₂ (pH 7.4). GABA_B responses were induced with a 30 s application of 100 μM baclofen. Solutions were delivered to a recording chamber using a gravity-driven perfusion system with exchange times of ~ 1 s. Cells were voltage-clamped at -60 mV using an Axopatch 200B amplifier (Molecular Devices). Patch pipettes with resistances of 3–7 M Ω were filled with an intracellular solution composed of 107.5 mM potassium gluconate, 32.5 mM KCl, 10 mM HEPES, 10 mM Tris phosphocreatine, 5 mM EGTA, 4 mM Na₂ATP, and 0.6 mM Na₂GTP (pH 7.2). Currents were sampled at 10 kHz and filtered using a low-pass Bessel (8-pole) at 2 kHz. Recordings were analyzed using Clampfit (Molecular Devices) and Prism (GraphPad). The number of experimental replicates per condition is as follows: 4 - KCTD, 2 +KCTD, 3 +EGFP-KCTD, 2 +EGFP-KCTD12-R257D, 2 +EGFP-KCTD12-R232D. The number of cells measured per condition is as follows: 13 -KCTD, 11 +KCTD, 13 +EGFP-KCTD, 9 +EGFP-KCTD12-R257D, 6 +EGFP-KCTD12-R232D. Relative desensitization of the baclofen-induced response was calculated as follows: $1 - (\text{amplitude prior to baclofen washout})/(\text{peak amplitude following baclofen application})$. Error bars indicate SEM, and statistical significance was assessed using a two-tailed parametric Student's t-test with a threshold of $p < 0.05$.

Data Availability Statement

The refined coordinates and structure factors for the KCTD16_{BTB}/GABA_{B2} peptide complex and KCTD12_{H1}/Gβ₁γ₂ complex have been deposited in the protein data bank under the accession codes 6M8R and 6M8S respectively.

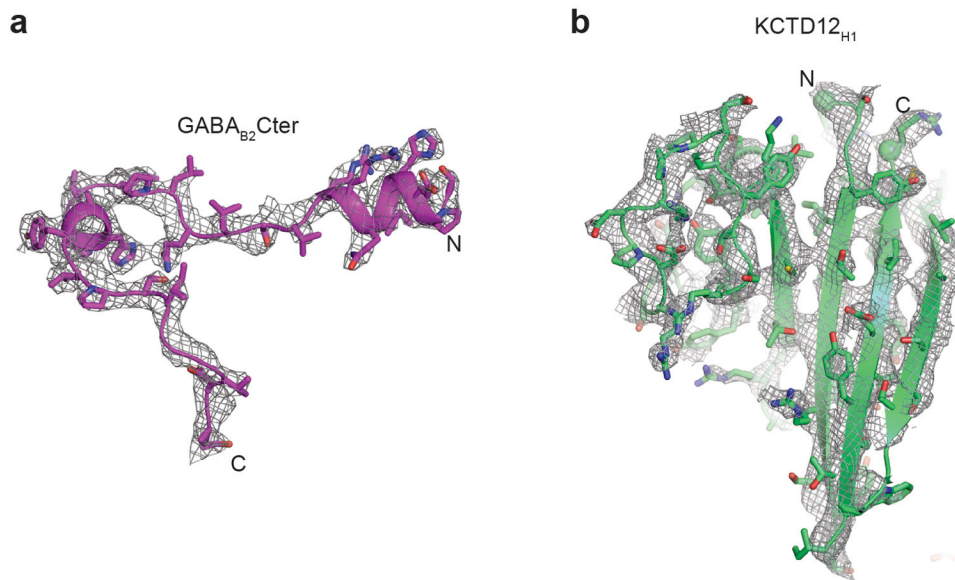
Extended Data



Extended Data Figure 1 | Mapping the GABA_{B2} binding region of BTB domain

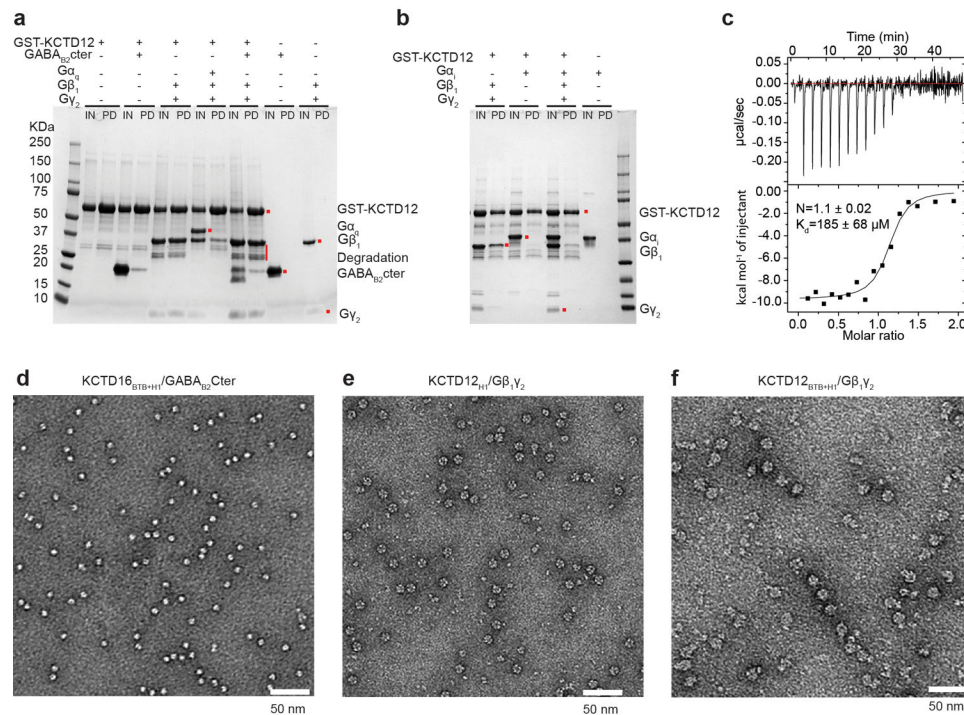
a, His6-SMT3-tagged KCTD16_{BTB} or KCTD12_{BTB} and His6-GST-tagged GABA_{B2} peptides were co-expressed in *E. coli* and purified with nickel affinity chromatography. Purified protein were loaded as input for pull-down with glutathione sepharose beads. Glutathione input (IN) and pull-down (PD) fractions were analyzed by SDS-PAGE and Coomassie blue staining. **b**, His6-GST-tagged GABA_{B2} and untagged KCTD16_{BTB} were co-expressed in *E. coli*. Clarified lysate was pulled down with glutathione Sepharose beads and eluate was analyzed by SDS-PAGE and Coomassie blue staining. **c**, Structural superposition of the KCTD16_{BTB} structure in GABA_{B2} peptide-free (grey) and bound state (red; PDB ID 5A15). **d**, His6-SMT3-tagged KCTD16_{BTB} wild-type (WT) or F80A mutant and His6-GST-tagged GABA_{B2} peptides were co-expressed and purified with nickel affinity. The eluate was treated with ULP1 to cleave SMT3 tag (IN) prior to glutathione Sepharose beads pull-

down. **e**, Sequence alignment of the BTB domain of KCTD family members from *Homo sapiens*. Residues with 98%, 80% and 60% similarity are shown in black, grey, and light grey, respectively.



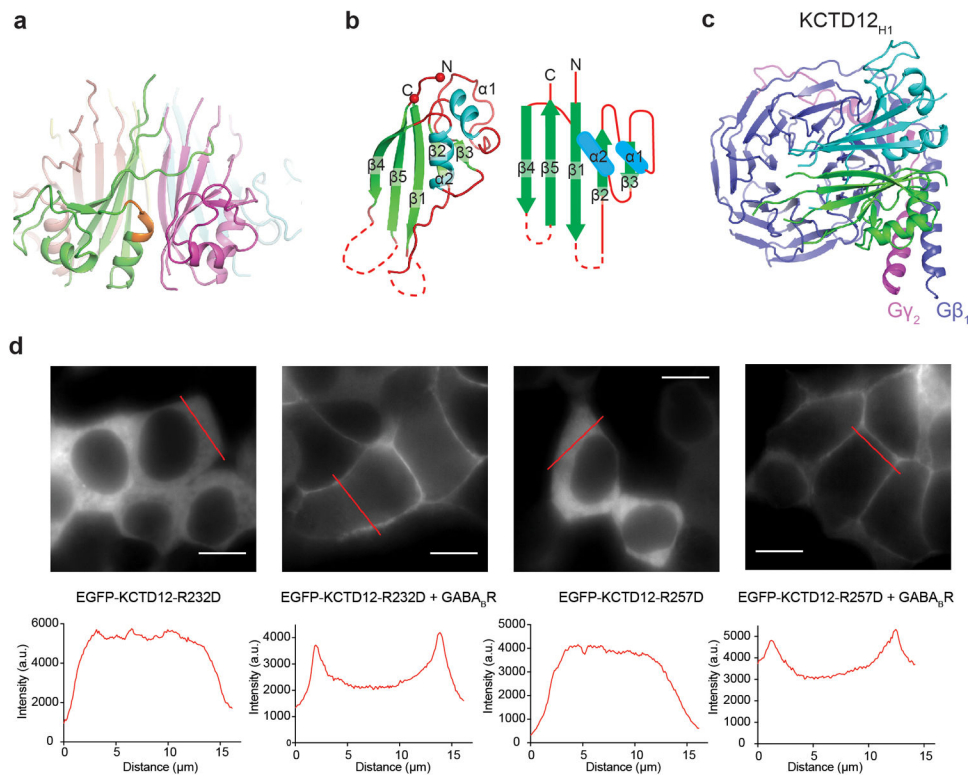
Extended Data Figure 2 |. Electron density maps

a, Composite omit $2F_o - F_c$ electron density map contoured at 1.0σ for GABA_{B2} peptide in KCTD16_{BTB}/GABA_{B2} peptide complex structure. **b**, Composite omit $2F_o - F_c$ electron density map contoured at 1.0σ for KCTD12_{H1} domain in KCTD12_{H1} - G $\beta_1\gamma_2$ complex structure.



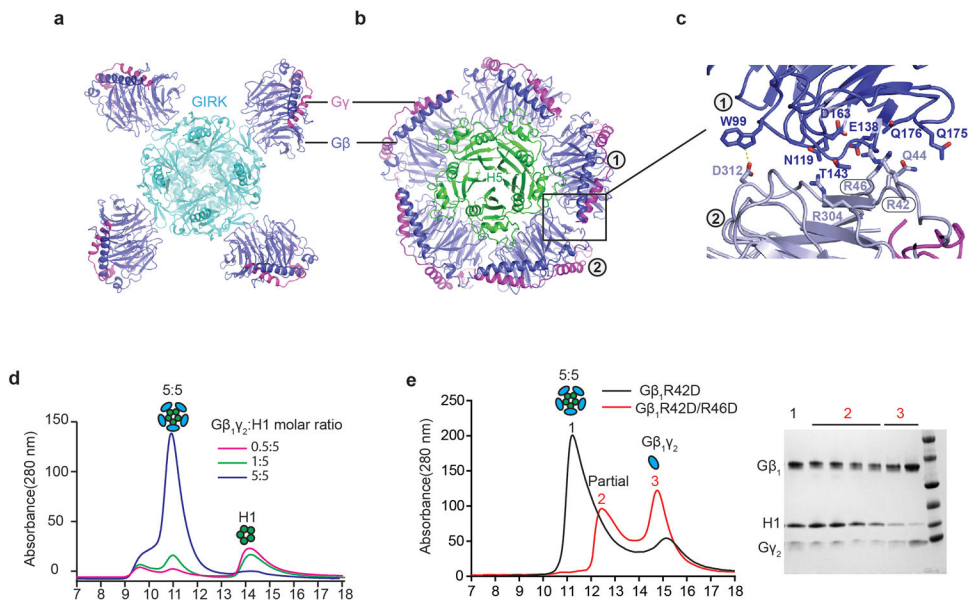
Extended Data Figure 3 | Representative negative stain electron micrographs

a, The full SDS-PAGE gel of pull-down experiment shown in Figure 2a. b, $G\alpha_i$ competes with KCTD12 for binding $G\beta_1\gamma_2$. Pull-down experiments were carried out in the same way as Figure 2a except that $G\alpha_q$ subtype instead of $G\alpha_i$ was used. c, Isothermal titration calorimetry affinity measurement for KCTD12_{H1} binding to $G\beta_1\gamma_2$. d, Representative image of KCTD16_{BTB+H1}/GABA_{B2}Cter. e, Representative image of KCTD12_{H1}/G $\beta_1\gamma_2$. f, Representative image of KCTD12_{BTB+H1}/GABA_{B2}Cter/G $\beta_1\gamma_2$.



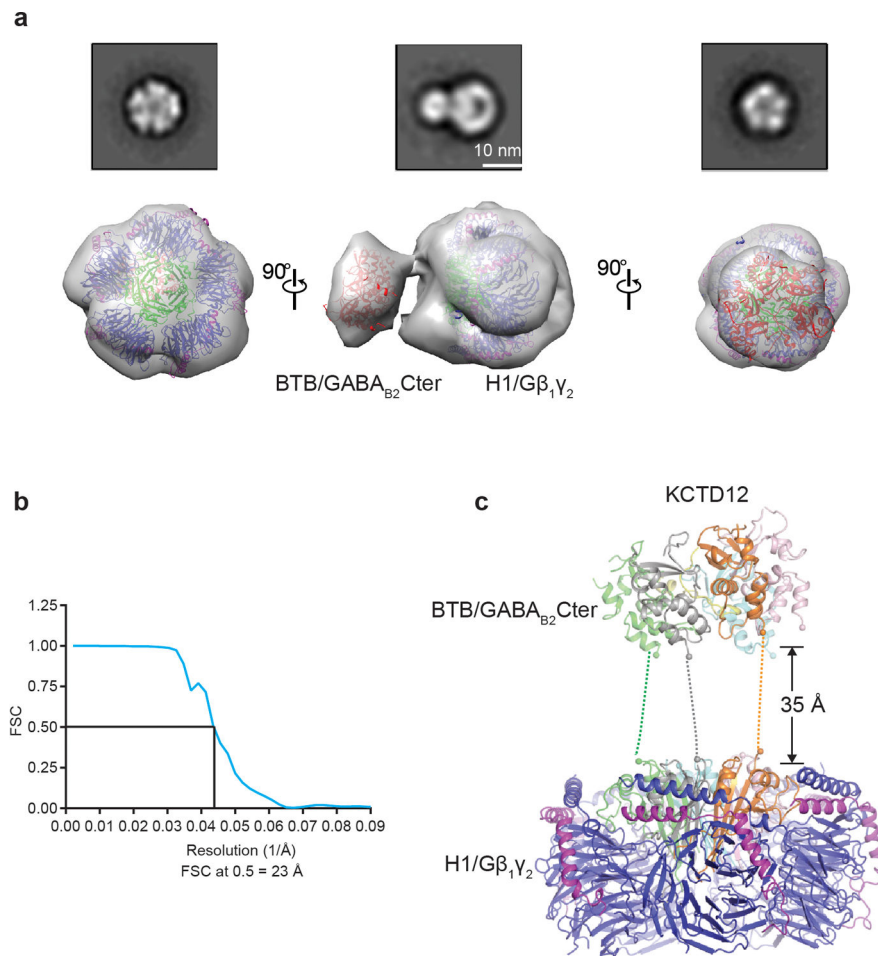
Extended Data Figure 4 | 3D negative stain EM reconstruction of the KCTD12 full-length complex including KCTD12 full length, GABA_{B2}Cter and Gβ₁γ₂

a, Three different views of the three-dimensional reconstruction of full length KCTD12-Gβ₁γ₂ complex with KCTD16_{BTB}-GABA_{B2} peptide complex (red) and KCTD12_{H1}-Gβ₁γ₂ complex (blue-magenta) crystal structures docked into the negative stain electron microscopy envelope. Negative stain 2D class averages are reproduced from Figure 2b for reference. **b**, The Fourier shell correlation (FSC) curve as a function of spatial frequency for negative staining EM map. Resolution is indicated below. **c**, Structure of full-length KCTD12 complex. The BTB domain is separated from H1 domain by 35 Å. Dashed lines represent the linker sequence between BTB and H1 domains.



Extended Data Figure 5 | Structural and functional analysis of H1 domain.

a, Ribbon representation of KCTD12 H1 domain. The NFLEQ motif important for desensitization is colored orange. **b**, Ribbon representation and topology map of the KCTD12 H1 monomer. Secondary structure elements are labeled. **c**, Ribbon representation of two KCTD12_{H1} subunits (green and cyan) and Gβ₁γ₂. **d**, Subcellular localization of eGFP-KCTD12-R232D and R257D mutants with or without GABA_B receptor



Extended Data Figure 7 | A model for GABA_B signaling and desensitization.

a, Agonist binding to GABA_{B1} receptor causes the dissociation of Gβγ heterodimer from Gα. Four copies of Gβγ bind to a GIRK channel tetramer, resulting in channel activation. Afterwards, KCTD bound to the GABA_{B2} C-terminus strips four copies of Gβγ from the GIRK channel and deactivates it. Following nucleotide hydrolysis, GDP-bound Gα binds to Gβγ, sequestering it from KCTD and priming the system for another signaling cycle. **b**, Calculated energies for the series of progressively tighter binding events are commensurate with the approximate energy released by GTP hydrolysis.

Extended Data Table 1 |

Crystallographic statistics

	KCTD16 _{BTB} /GABA _{B2} Cter	KCTD12 _{H1} /Gβ ₁ γ ₂
Data collection		
Space group	<i>P</i> 2 ₁	<i>P</i> 2 ₁ 2 ₁ 2 ₁
Cell dimensions		
<i>a</i> , <i>b</i> , <i>c</i> (Å)	92.5, 65.1, 114.1	109.1, 122.0, 206.4
α, β, γ (°)	90.0, 99.6, 90.0	90.0, 90.0, 90.0

Resolution (Å)	50 – 3.2 (3.28 – 3.20)	50 – 3.71 (3.80 – 3.71)
R_{merge} (%)	33.2 (99.7)	31.2(105.9)
CC1/2 (%)	92.6 (56.1)	96.2 (52.0)
$I/\sigma I$	3.4 (0.6)	3.56 (1.09)
Completeness (%)	99.2 (96.7)	99.0 (97.6)
Redundancy	3.3 (2.7)	3.9 (4.0)
Refinement		
Resolution (Å)	38.6–3.2 (3.29–3.20)	48.4–3.71 (3.76–3.71)
No. reflections	22002	29614
$R_{\text{work}} / R_{\text{free}}$ (%)	23.6 / 27.6	25.6 / 28.1
No. atoms	8462	18990
Protein	8462	18990
Ligand/ion	0	0
Water	0	0
B -factors	57.3	93.0
Protein	57.3	93.0
Ligand/ion	N/A	N/A
Water	N/A	N/A
R.m.s. deviations		
Bond lengths (Å)	0.005	0.003
Bond angles (°)	1.095	0.764

*Values in parentheses are for highest shell.

Supplementary Material

Refer to Web version on PubMed Central for supplementary material.

Acknowledgements

We thank Kelly Arnett and the Harvard Medical School Center for Macromolecular Interactions for assistance with biophysical measurements, Melissa Chambers at Harvard Cryo-Electron Microscopy center for EM training, and we thank Jiahao Liang and Aashish Manglik for providing purified $G\alpha_i$ protein. We also thank Hayden Schmidt for critical reading of the manuscript. Technical support for crystallographic software and computation was provided by SBGrid. Funding was provided by a Klingenstein-Simons Fellowship (A.C.K.), the Smith Family Foundation (A.C.K.), grant R35 GM124731 from the National Institute of General Medicine (J.L.) and an NSF Graduate Research Fellowship (N.A.).

REFERENCES

1. Pin JP & Bettler B Organization and functions of mGlu and GABAB receptor complexes. *Nature* 540, 60–68, doi:10.1038/nature20566 (2016). [PubMed: 27905440]
2. Froestl W Chemistry and pharmacology of GABAB receptor ligands. *Advances in pharmacology* (San Diego, Calif.) 58, 19–62, doi:10.1016/s1054-3589(10)58002-5 (2010).
3. Schwenk J et al. Native GABA(B) receptors are heteromultimers with a family of auxiliary subunits. *Nature* 465, 231–235, doi:10.1038/nature08964 (2010). [PubMed: 20400944]
4. Turecek R et al. Auxiliary GABAB receptor subunits uncouple G protein betagamma subunits from effector channels to induce desensitization. *Neuron* 82, 1032–1044, doi:10.1016/j.neuron.2014.04.015 (2014). [PubMed: 24836506]

5. Ivankova K et al. Up-regulation of GABA(B) receptor signaling by constitutive assembly with the K + channel tetramerization domain-containing protein 12 (KCTD12). *J Biol Chem* 288, 24848–24856, doi:10.1074/jbc.M113.476770 (2013). [PubMed: 23843457]
6. Marshall FH, Jones KA, Kaupmann K & Bettler B GABAB receptors - the first 7TM heterodimers. *Trends Pharmacol Sci* 20, 396–399 (1999). [PubMed: 10498952]
7. Geng Y et al. Structure and functional interaction of the extracellular domain of human GABA(B) receptor GBR2. *Nature neuroscience* 15, 970–978, doi:10.1038/nn.3133 (2012). [PubMed: 22660477]
8. Geng Y, Bush M, Mosyak L, Wang F & Fan QR Structural mechanism of ligand activation in human GABA(B) receptor. *Nature* 504, 254–259, doi:10.1038/nature12725 (2013). [PubMed: 24305054]
9. Bettler B & Tiao JY Molecular diversity, trafficking and subcellular localization of GABAB receptors. *Pharmacol Ther* 110, 533–543, doi:10.1016/j.pharmthera.2006.03.006 (2006). [PubMed: 16644017]
10. Gassmann M & Bettler B Regulation of neuronal GABA(B) receptor functions by subunit composition. *Nature reviews. Neuroscience* 13, 380–394, doi:10.1038/nrn3249 (2012). [PubMed: 22595784]
11. Padgett CL & Slesinger PA GABAB receptor coupling to G-proteins and ion channels. *Advances in pharmacology (San Diego, Calif.)* 58, 123–147, doi:10.1016/s1054-3589(10)58006-2 (2010).
12. Huang CL, Slesinger PA, Casey PJ, Jan YN & Jan LY Evidence that direct binding of G beta gamma to the GIRK1 G protein-gated inwardly rectifying K+ channel is important for channel activation. *Neuron* 15, 1133–1143 (1995). [PubMed: 7576656]
13. Correale S et al. A biophysical characterization of the folded domains of KCTD12: insights into interaction with the GABAB2 receptor. *Journal of molecular recognition : JMR* 26, 488–495, doi: 10.1002/jmr.2291 (2013). [PubMed: 23996491]
14. Lee MT et al. Genome-wide association study of bipolar I disorder in the Han Chinese population. *Molecular psychiatry* 16, 548–556, doi:10.1038/mp.2010.43 (2011). [PubMed: 20386566]
15. Metz M, Gassmann M, Fakler B, Schaeren-Wiemers N & Bettler B Distribution of the auxiliary GABAB receptor subunits KCTD8, 12, 12b, and 16 in the mouse brain. *The Journal of comparative neurology* 519, 1435–1454, doi:10.1002/cne.22610 (2011). [PubMed: 21452234]
16. Schwenk J et al. Modular composition and dynamics of native GABAB receptors identified by high-resolution proteomics. *Nature neuroscience* 19, 233–242, doi:10.1038/nn.4198 (2016). [PubMed: 26691831]
17. Pinkas DM et al. Structural complexity in the KCTD family of Cullin3-dependent E3 ubiquitin ligases. *The Biochemical journal* 474, 3747–3761, doi:10.1042/bcj20170527 (2017). [PubMed: 28963344]
18. Seddik R et al. Opposite effects of KCTD subunit domains on GABA(B) receptor-mediated desensitization. *J Biol Chem* 287, 39869–39877, doi:10.1074/jbc.M112.412767 (2012). [PubMed: 23035119]
19. Whorton MR & MacKinnon R X-ray structure of the mammalian GIRK2-beta gamma G-protein complex. *Nature* 498, 190–197, doi:10.1038/nature12241 (2013). [PubMed: 23739333]
20. Wang W, Touhara KK, Weir K, Bean BP & MacKinnon R Cooperative regulation by G proteins and Na(+) of neuronal GIRK2 K(+) channels. *Elife* 5, doi:10.7554/eLife.15751 (2016).
21. Yokogawa M, Osawa M, Takeuchi K, Mase Y & Shimada I NMR analyses of the Gbetagamma binding and conformational rearrangements of the cytoplasmic pore of G protein-activated inwardly rectifying potassium channel 1 (GIRK1). *J Biol Chem* 286, 2215–2223, doi:10.1074/jbc.M110.160754 (2011). [PubMed: 21075842]
22. Sarvazyan NA, Remmers AE & Neubig RR Determinants of gi1 alpha and beta gamma binding. Measuring high affinity interactions in a lipid environment using flow cytometry. *J Biol Chem* 273, 7934–7940 (1998). [PubMed: 9525890]
23. Dror RO et al. SIGNAL TRANSDUCTION. Structural basis for nucleotide exchange in heterotrimeric G proteins. *Science* 348, 1361–1365, doi:10.1126/science.aaa5264 (2015). [PubMed: 26089515]

24. Zheng S & Ye K Purification, crystallization and preliminary X-ray diffraction analysis of Imp3 in complex with an Mpp10 peptide involved in yeast ribosome biogenesis. *Acta Crystallogr F Struct Biol Commun* 70, 918–921, doi:10.1107/S2053230X14010905 (2014). [PubMed: 25005089]
25. Otwinowski Z & Minor W Processing of X-ray diffraction data collected in oscillation mode. *Methods Enzymol* 276, 307–326 (1997).
26. Adams PD et al. PHENIX: a comprehensive Python-based system for macromolecular structure solution. *Acta Crystallogr D Biol Crystallogr* 66, 213–221, doi:10.1107/S0907444909052925 (2010). [PubMed: 20124702]
27. Lodowski DT, Pitcher JA, Capel WD, Lefkowitz RJ & Tesmer JJ Keeping G proteins at bay: a complex between G protein-coupled receptor kinase 2 and Gbetagamma. *Science* 300, 1256–1262, doi:10.1126/science.1082348 (2003). [PubMed: 12764189]
28. Emsley P & Cowtan K Coot: model-building tools for molecular graphics. *Acta Crystallogr D Biol Crystallogr* 60, 2126–2132, doi:10.1107/s0907444904019158 (2004). [PubMed: 15572765]
29. Afonine PV et al. Towards automated crystallographic structure refinement with phenix.refine. *Acta Crystallogr D Biol Crystallogr* 68, 352–367, doi:10.1107/s0907444912001308 (2012). [PubMed: 22505256]
30. Rees I, Langley E, Chiu W & Ludtke SJ EMEN2: an object oriented database and electronic lab notebook. *Microsc Microanal* 19, 1–10, doi:10.1017/S1431927612014043 (2013).
31. Scheres SH RELION: implementation of a Bayesian approach to cryo-EM structure determination. *J Struct Biol* 180, 519–530, doi:10.1016/j.jsb.2012.09.006 (2012). [PubMed: 23000701]
32. Grant T, Rohou A & Grigorieff N cisTEM, user-friendly software for single-particle image processing. *Elife* 7, doi:10.7554/eLife.35383 (2018).

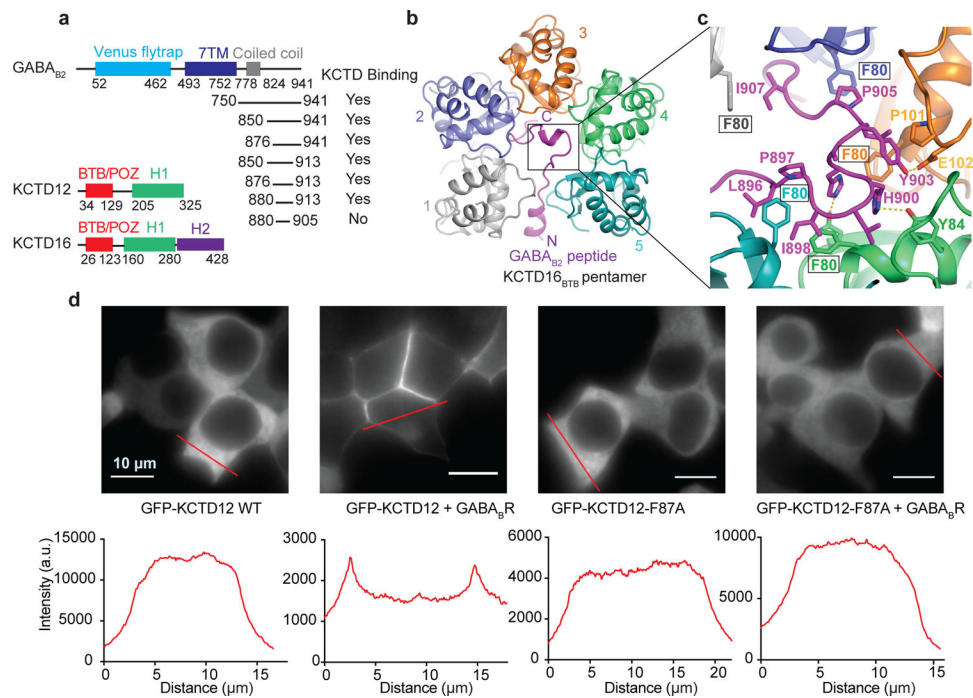


Figure 1 |. Crystal structure of KCTD16 BTB domain in complex with GABA_{B2} C-terminal peptide.

a, Schematic representation of the domain organization of GABA_{B2} receptor, KCTD12 and KCTD16. Summary of GST pull-down results with GST-tagged GABA_{B2} fragments and KCTD16 BTB domain. **b**, Ribbon representation of the KCTD16_{BTB}/GABA_{B2} peptide complex structure. **c**, Detailed view of the interface indicated on the structure by the black box in panel (b). **d**, Subcellular localization of GFP-KCTD12 or GFP-KCTD12-F87A (equivalent to F80A in KCTD16) with or without GABA_B receptor in HEK293T cells.

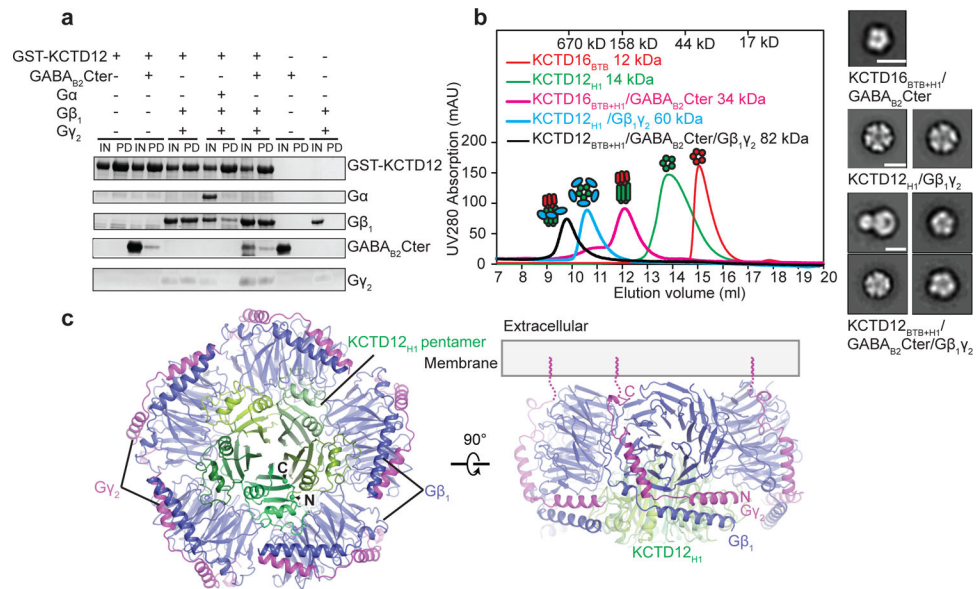


Figure 2 | Crystal structure of KCTD12 H1 domain and Gβ₁γ₂ complex.

a, GST pull-down experiment. The input (IN) and pull-down (PD) fractions were separated by SDS-PAGE and stained with Coomassie Blue. **b**, Size exclusion chromatography analysis of individual domains and complexes. KCTD16_{BTB+H1} and KCTD12_{BTB+H1} contain both BTB and H1 domain. Representative views of negative stain EM 2D class averages for each complex are shown on the right. The scale bar in each panel represents 10 nm. **c**, Orthogonal views of the crystal structure of the KCTD12 H1 pentamer in complex with five copies of Gβ₁γ₂ heterodimer colored by subunit.

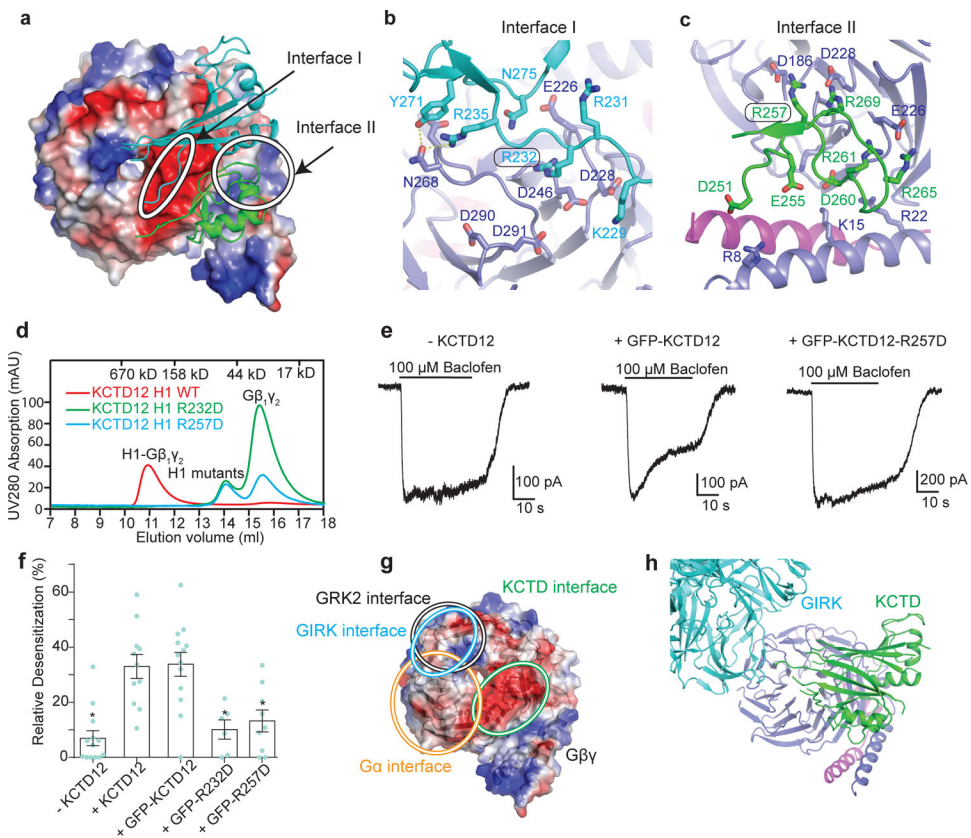


Figure 3 | Mechanism of the $G\beta_1\gamma_2$ recognition by KCTD12_{H1} domain.

a, The two KCTD12_{H1} subunits contact distinct surfaces of $G\beta_1\gamma_2$, denoted “interface I” and “interface II”. **b**, Interactions in interface I. **c**, Interactions in interface II. **d**, KCTD12_{H1} R232D or R257D mutations abolish interaction with $G\beta_1\gamma_2$ in size exclusion. **e**, Whole-cell patch clamp GIRK current traces recorded from CHO cells co-expressing GABA_B receptor, GIRK1 and wild-type or mutant KCTD12. **f**, Relative desensitization levels shown as means \pm SEM. Each data point is from one cell. **g**, KCTD12, GRK2, GIRK and G α binding interfaces circled on $G\beta_1\gamma_2$. **h**, The GIRK channel shows a distinct interface from KCTD12_{H1} on $G\beta$.

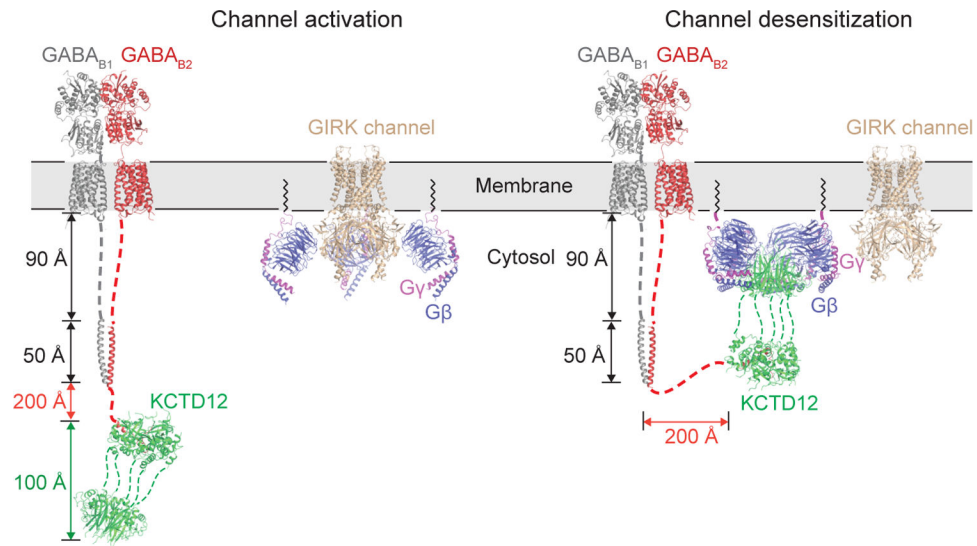


Figure 4 | Proposed mechanism for GIRK channel desensitization.

GABA_{B2} receptor is tethered via a long linker to KCTD12, which may allow it to diffuse far from the membrane. Gβγ subunits are released from Gα_{i/o} by activated receptor, but are membrane-tethered and rapidly associate with GIRK channels. Association of KCTD12 with a single GIRK-bound Gβγ subunit tethers KCTD12 to the membrane, allowing it to rapidly strip remaining Gβγ subunits from the activated channel. Note that distances cannot be shown to scale due to the extreme length of the tether between the GABA_{B2} transmembrane domain and the KCTD12 binding site.